PERGAMON

Aerosol Science 33 (2002) 1235–1259

Journal of
Aerosol Science

www.elsevier.com/locate/jaerosci

Relationship of sampling efficiency for manikin-mounted personal samplers to efficiency measurements made independent of manikin

Jerome P. Smith[a,*], Aaron J. Bird[b,c]

[a] *Centers for Disease Control and Prevention, National Institute for Occupational Safety and Health, Division of Applied Research and Technology, 4676 Columbia Parkway, Cincinnati, OH 45226, USA*
[b] *Centers for Disease Control and Prevention, National Institute for Occupational Safety and Health, Health Effects Laboratory Division, 1095 Willowdale Road, Morgantown, WV 26505, USA*
[c] *Industrial and Management Systems Engineering Department, P.O. Box 6107, West Virginia University, Morgantown, WV 26506, USA*

Received 15 May 2001; received in revised form 15 April 2002; accepted 17 April 2002

Abstract

The goal of this study was to determine if measurement of the airflow approaching manikin-mounted personal samplers can be used to predict their sampling efficiency using efficiency measurements made independently of the manikin. The first part of the work involved the determination of the velocity and direction of airflow at specific locations (where personal samplers would be located) around a human-like manikin by using laser-Doppler velocimetry (LDV) at two wind speeds and three orientations of the manikin with respect to the wind. Sampling-efficiency measurements for two personal samplers, the IOM (SKC, Inc., Eighty-Four, PA) and GSP (Strohlein GmbH and Co., Kaarst, Germany) for a 70 μm (mass median diameter) aerosol were made both independently of the manikin for a range of wind speeds and directions and while mounted on the manikin for the wind speeds and directions studied by LDV. The efficiency measurements made independently of the manikin were adjusted by using the local-manikin concentration experienced by the sampler to calculate an approximated efficiency for manikin-mounted personal samplers that experienced a similar wind speed and direction. The approximated efficiency agreed with the measured efficiency of the manikin-mounted samplers when the manikin faced the wind or was at 90° to the wind. Some assumptions were required to obtain agreement when the manikin was at 180° to the wind probably due to the turbulent nature of the flow with the manikin at this angle to the wind. This technique may be useful in simplifying testing procedures and in developing performance criteria for inhalable dust samplers since clearly defined test conditions can be specified. Published by Elsevier Science Ltd.

Keywords: Personal samplers; Manikin-mounted samplers; Airflow behavior

* Corresponding author. Tel.: +1-513-533-8394.
E-mail address: jps3@cdc.gov (J.P. Smith).

0021-8502/02/$ - see front matter. Published by Elsevier Science Ltd.
PII: S0021-8502(02)00068-X

1. Introduction

When a personal sampler is placed on a worker, it is expected that the airflow around the sampler will be influenced by the following factors: its placement, the direction and speed of the local free-stream airflow, the worker's motion, and the occupational environment. Testing of personal inhalable dust samplers has therefore been done by placing the samplers on a manikin and studying the efficiency of the samplers as a function of wind speed and direction approaching the manikin. There have been a number of studies of sampling efficiency conducted for manikin-mounted samplers (e.g. Wood & Birkett, 1979; Mark & Vincent, 1986; Hinds & Kuo, 1995; Hinds, Tatyan, & Kennedy, 2001). In a recent study, a large number of commonly used sampler types were studied and the manikin was rotated continuously over 360° to simulate the performance of samplers while mounted on workers (Kenny et al., 1997). Kenny's study found, in general, that the samplers performed best at low windspeeds. Alternately, samplers have also been tested while mounted on a fixed manikin (Chung, Ogden, & Vaughan, 1987). More recent studies give data and techniques for the performance of manikin-mounted samplers in still air (Kenny, Aitken, Baldwin, Beaumont, & Maynard, 1999; Aitken, Baldwin, Beaumont, Kenny, & Maynard, 1999). An additional study sought to develop a system that even more closely resembled sampler use on workers in which Botham, Hughson, Vincent, and Mark (1991) used a breathing manikin, having a moveable torso and arms, to approximate airflow conditions in a workplace. It has been found that different types of personal inhalable dust samplers gave different values when used in the workplace (Tsai, Vincent, & Mark, 1996; Tatum, Ray, & Rovell-Rixx, 2001). A number of types of personal inhalable dust samplers have also been tested recently in free air without a manikin (Li, Lundgren, & Rovell-Rixx, 2000) and found to vary in efficiency. The amount of difference depended on the wind speed, direction, and particle size. The value of the sampling efficiency of a personal sampler, relative to an isokinetic reference sampler, was different when the personal samplers were mounted on a manikin, compared to when they were suspended in free air (Buchan, Soderholm, & Tillery, 1986). Recent data indicates that sampling efficiencies measured in the laboratory may not accurately reflect sampling efficiencies observed in the field (Liden, Juringe, & Gudmundsson, 2000).

A number of studies have also been performed to numerically simulate the airflow approaching samplers and sampling characteristics of manikin-mounted samplers (e.g. Wen & Ingham, 2000; Dunnett & Vincent, 2000; Dunnett, 1997; Chung & Dunn-Rankin, 1997; Dunnett, 1999). Most of these studies have simulated the sampler/body system as a simple geometric figure with aspiration taking place within this geometry. These studies have led to a better understanding of air flow approaching samplers and factors that determine sampler performance.

If flow approaching samplers mounted on a manikin were better understood then factors affecting performance could be better predicted. A study addressing sampler placement was done by Rodes, Kamens, and Wiener (1995), who found that a stagnation region of lower velocity existed in the center of the front of a manikin, while it was facing the wind, and that some regions with higher velocity than freestream existed outside this stagnation region, which is expected from fluid dynamics considerations. In other studies, flow in front of the manikin, with the back of the manikin facing the wind, was characterized in terms of vortex shedding and downwash conditions, formed when the freestream air flowed around the manikin (Kim & Flynn, 1991; Flynn, Chen, Kim, & Muthedath, 1995; Flynn & Ljungqvist, 1995). It has also been found that flow in the breathing zone can be affected by thermal effects under low-wind-speed conditions (Johnson, Fletcher, & Saunders,

1996) and by worker's motion (Botham et al., 1991). Each of these efforts serves to bring greater understanding to the physics of collection efficiency for worker-mounted samplers. To add to this knowledge, laser-Doppler velocimetry (LDV) measurements and sampler collection efficiency experiments, which are described in this paper, were combined to investigate specific airflow conditions around manikin-mounted samplers and the effect on sampling efficiency.

The overall goal of this research was to determine if an understanding the airflow approaching samplers on a manikin can be used to predict the sampling efficiency of manikin-mounted samplers. Two different samplers were studied (IOM Inhalable Sampler and GSP). The IOM and GSP were chosen because they are commonly used personal samplers, have simple round inlets, have inlets at different distances from the manikin (0.07 m for GSP and 0.03 m for IOM) and have different inlet velocities (0.19 m/s for IOM and 1.32 m/s for GSP). The first part of the study used LDV measurements as a basis to aid in understanding airflow behavior near the inlets of samplers and the second part studied the sampling efficiency of the samplers independently of the manikin and while mounted on the manikin. The sampling efficiency determined independently of manikin was used to predict those of samplers on the manikin by examining the airflow approaching manikin-mounted samplers.

2. Experimental setup and method

2.1. Wind tunnel and manikins

Air velocity at various positions around the manikin was measured in a wind tunnel, (1.22 m high by 1.83 m wide, previously described by Smith, Bartley, and Watkins (1999) at wind velocities of 0.5 and 2 m/s. These wind velocities were chosen because they represent a range of airflow velocities likely to occur in the workplace (Baldwin & Maynard, 1998). Fig. 1 shows the overall configuration of the test section of the wind tunnel with the large and small particle generation systems. The large particle generation system distributed the aerosol over an area including the manikin and reference samplers and was used to study sampling efficiency of manikin-mounted samplers and samplers in free air for large particles (Smith et al., 1999). The small particle generation system was used to generate particles for the LDV measurements. The coordinate system (x, y, z) used to measure distances around the manikin and the components of velocity (U, W, V) measured by the LDV system in relation to the wind tunnel and manikin are also shown. The free-stream turbulence intensity in the test section of the wind tunnel was 3–4% and appeared to be isotropic as measured by the LDV system.

A full size, top half (waist up) of a tailor's manikin (Fig. 2) was used in this study. This manikin was non-breathing. Velocity measurements were taken at the center of the chest and positions 0.1 m to the right and left of center, at heights of 0.38 and 0.43 m above the floor of the wind tunnel. Velocity measurements were taken in the face area, between the nose and mouth, at the center, and at 0.05 m to the right and left of center at two heights covering the mouth and nose areas. These velocity measurements using the full-size manikin were made at orientations of 0°, 90°, and 180° angles to the wind. The manikin leaned slightly to the right and the head was turned slightly to the left. In addition, the right forearm extended slightly in front of the manikin and the left forearm was slightly behind, making the manikin somewhat unsymmetrical. No samplers were attached to the manikin while the LDV measurements were taken.

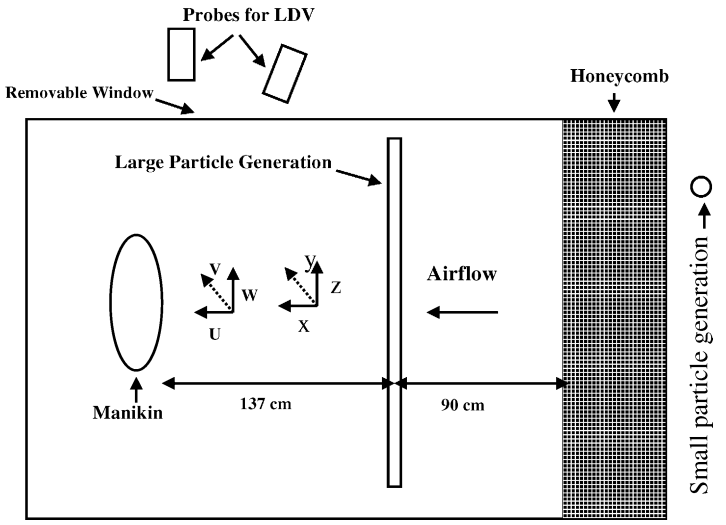

Fig. 1. Schematic (top view) of test section of wind tunnel showing location of manikin, LDV probes, large and small particle generation systems, coordinate system for distance measurement (x, y, z) and components of velocity (U, V, W).

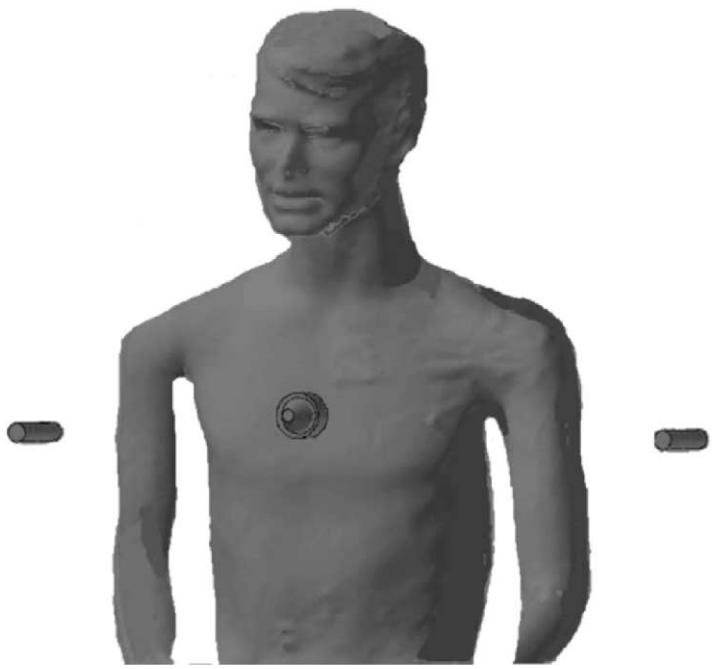

Fig. 2. Computer rendering of full-size manikin used in LDV and sampler efficiency measurements, showing locations of isokinetic samplers and GSP sampler at $z = 0$ center location and height of $y = 0.43$ m.

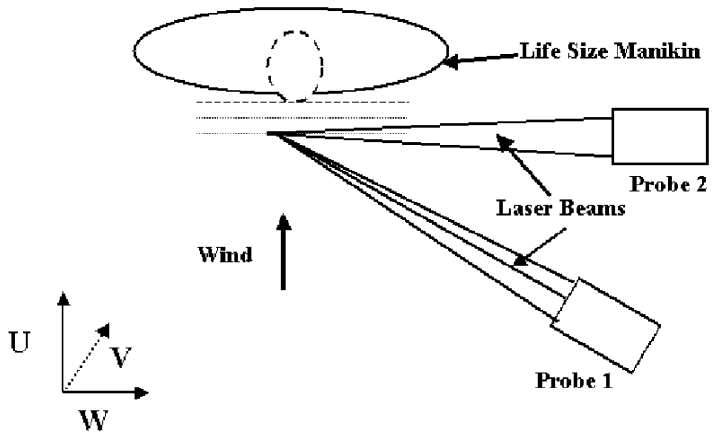

Fig. 3. Laser beam placement around manikin. For LDV measurements.

2.2. Laser doppler velocimetry

The air-velocity measurements were performed using LDV (3D Fiberflow System, Dantec Measurement Technology Inc, Mahwah, NJ) which had two probes located outside of the wind tunnel that allowed measurement of the three components of velocity. The LDV system determined the velocity by measuring transit times of particles moving through an interference pattern formed by the intersection of two laser beams. Small particles of corn-oil aerosol, 0.7 μm count median aerodynamic diameter (CMAD), were used as the flow-indicating seed aerosol (Smith et al., 1999).

The three orthogonal components of velocity measured were the following: U, the horizontal component along the main axis of the wind tunnel (x direction); V, the vertical component (y direction); and W, a horizontal component across the width of the tunnel (z direction). Two intersecting beams were transmitted over three different wavelengths, for a total of six beams used for the measurements (Fig. 3). Probe 1 used 514 nm wavelength beams for measurement of the U component (horizontal, downwind) and 488 nm for measurement of the V component. Probe 2 (477 nm) was placed at an angle of approximately 30° to probe 1, and their measurements were combined to obtain the U component along the axis of the wind tunnel and W component in the lateral direction. The configuration shown in Fig. 3 was used for measurements when the manikin was at a 0° angle with respect to the wind. At other angles, the configuration was slightly different to allow the laser beams to reach the desired locations for measurements.

Velocity measurements on the full-size manikin were taken at 0.01 m intervals, starting about 0.20 m from the manikin and ending at a point as close to the surface as possible. The starting locations of the measurements were chosen arbitrarily; however, the x direction scan toward the surface of the manikin was sequential, allowing the possible introduction of some systematic error. Specifically, the data collected was the mean and RMS fluctuation of the velocity about the mean velocity for the U, V, and W components. A minimum of 50 data points were collected in most cases, and the measurement time was usually at least 10 s. Difficulties that prevented collection of 50 data points or measurements for at least 10 s, which was a rare occurrence, were attributed to

high reflectivity of the manikin's surface in areas where velocity fluctuation was high and random. In addition, there were difficulties in measuring at all locations due to blockages of regions of the manikin at certain angles studied.

3. Sampling efficiency measurements

For the sampling-efficiency experiments conducted in this study, a large particle generation system making use of a Palas, rotating-brush aerosol generator (Model RBG-1000, Palas GmbH, Karlsruhe, Germany) and a mechanical aerosol distributor were employed to uniformly deliver particles to the test area (position shown in Fig. 1). The aerosol distribution system previously described by Smith et al. (1999), was modified from its original arrangement by moving the two-axis positioning system to the roof of the wind tunnel. The generated aerosol was carried into the wind tunnel through a vertical 1.27 cm, outside diameter, rigid stainless steel tube, the end of which was attached to a horizontal nozzle in the wind tunnel. The flow exited the nozzle 180° to the flow in the wind tunnel, and the charge on the aerosol was reduced by exposing it to a bipolar ion source using separate adjustable corona discharges to produce positive and negative ions (Smith et al., 1999). The rigid tube and nozzle were moved in two dimensions (up and down, side to side) so the nozzle uniformly scanned the measurement area. The aerosol used in these experiments was a 240-grit graded aluminum oxide powder. Its mass median diameter was determined by sedimentation analysis to be 70 μm, and had a geometric standard deviation of 1.35 (Mark, Vincent, & Witherspoon, 1985).

The manikin used in this part of the study was the same as that used for the laser-Doppler measurements. Samplers were mounted on the manikin at a height of 0.41 m from the floor of the tunnel at the center position, as well as 0.10 m right and left of center. To determine the reference ambient concentration, free-stream reference samplers were placed at a height of 0.41 m above the floor of the tunnel and on the right and left about 0.3 m away from the manikin where flow disturbance due to the manikin was minimal or nonexistent.

The samplers used in this experiment included the commercially available GSP (Strohlein GmbH and Co., Kaarst, Germany) and the IOM (SKC, Inc., Eighty-Four, PA) personal samplers, thin-walled reference samplers, and near-body reference samplers. The GSP has an inlet length of 0.075 m and a 0.0075 m diameter inlet located at the apex of a cone. The IOM inhalable samplers has an inlet length of 0.03 m and an inlet diameter of 0.015 m. With the IOM sampler the filter of the sampler is contained in an internal cassette that includes the inlet of sampler (Mark & Vincent, 1986) This cassette is weighed together with the filter and thus all dust entering the inlet of the sampler is weighed. Stainless steel cassettes were used due to mass stability problems with plastic cassettes (Smith, Bartley, & Kennedy, 1998). With the GSP samplers, the filters were weighed after the dust on the plastic ring holding the filter was brushed off onto the filter. The thin-walled reference samplers, constructed to have little effect on the airflow, were 0.08 m long and had inlet diameters of approximately 0.01 m (Smith et al., 1999) and were used to determine the reference concentration. With the thin-walled reference sampler, the dust collected on the filter was weighed and the dust collected in the inlet was washed out and weighed separately (Smith et al., 1999). In this way, all the dust entering the inlet of the sampler was weighed. The near-body reference samplers were used to estimate the concentration near the manikin where personal samplers were located. The near-body reference samplers, that were used to measure concentration where the flow was straight into the

chest area of the manikin, were 0.03 m and 0.08 m in length, respectively (to match the lengths of the inlets of the IOM and GSP), and were mounted against the manikin in a manner similar to the way an IOM sampler is worn by a worker. These near-body samplers had 0.0279 and 0.01 m diameter inlets and were also constructed to have minimal impact on the airflow behavior. At locations where the measured flow was not straight into the chest i.e. at an angle to the chest (e.g. positions right and left of center when the manikin faced the wind and with the manikin at 90 to the wind), a near-body reference sampler with a thin-walled inlet 0.08 m long and with a 0.01 m diameter inlet was used to estimate the concentration. In all cases, the direction of the near-body reference sampler matched the direction of the airflow and the inlet velocity matched the measured wind speed at the location on the manikin. In the same manner as the thin-walled reference sampler, the dust collected on the filter of the near-body reference sampler was weighed and the dust collected in the inlet was washed out and weighed separately so that all the dust entering the inlet of the sampler was weighed.

3.1. Definitions of independent, measured, and approximated efficiencies

The fundamental goal of this simplified procedure is the development of a method to allow for a sampling efficiency that is measured independently of the manikin to be related to the efficiency of a manikin-mounted sampler. Therefore, a simple relationship was developed between efficiency measured when the sampler was mounted on the manikin and that measured independently of the manikin.

First, to determine the efficiency independently of the manikin, $\mathrm{Effic}_{\mathrm{ind}}$, the aerosol concentration, measured by a personal sampler in freestream flow, $\mathrm{Conc}_{\mathrm{psi}}$, was divided by the ambient reference concentration, $\mathrm{Conc}_{\mathrm{ref}}$, which was determined by a thin-walled isokinetic/isoaxial reference sampler (Fig. 4A). This determination is done for the range of wind speeds and directions that the sampler experiences when mounted on the manikin

$$\mathrm{Effic}_{\mathrm{ind}} = \mathrm{Conc}_{\mathrm{psi}}/\mathrm{Conc}_{\mathrm{ref}}. \tag{1}$$

The measured sampler efficiency for manikin-mounted samplers, $\mathrm{Effic}_{\mathrm{meas}}$, was determined by dividing the concentration measured by the personal sampler on the manikin, $\mathrm{Concn}_{\mathrm{psm}}$, by the ambient reference concentration, $\mathrm{Conc}_{\mathrm{ref}}$ (Fig. 4B). The wind speed and direction experienced by the sampler may be different from free stream velocity and the local concentration may be different from that in the free stream.

$$\mathrm{Effic}_{\mathrm{meas}} = \mathrm{Conc}_{\mathrm{psm}}/\mathrm{Conc}_{\mathrm{ref}}. \tag{2}$$

If air velocity and direction used to determine $\mathrm{Effic}_{\mathrm{ind}}$ adequately simulate those that determine $\mathrm{Effic}_{\mathrm{meas}}$, then the samplers presumably sample with the same efficiency. However, the aerosol concentration sampled by the manikin-mounted sampler may be modified by the presence of the manikin. Therefore, the local-manikin concentration, $\mathrm{Conc}_{\mathrm{lm}}$, (Fig. 4C) is determined using the near-body reference samplers and may differ from $\mathrm{Conc}_{\mathrm{ref}}$. This can be adjusted by introducing a local manikin efficiency term, $\mathrm{Effic}_{\mathrm{lm}}$, in the following way:

$$\mathrm{Effic}_{\mathrm{lm}} = \mathrm{Conc}_{\mathrm{lm}}/\mathrm{Conc}_{\mathrm{ref}}, \tag{3}$$

where $\mathrm{Effic}_{\mathrm{lm}}$ is a measure of the efficiency of particle transport from the ambient freestream flow into various areas within the near-body region of the manikin.

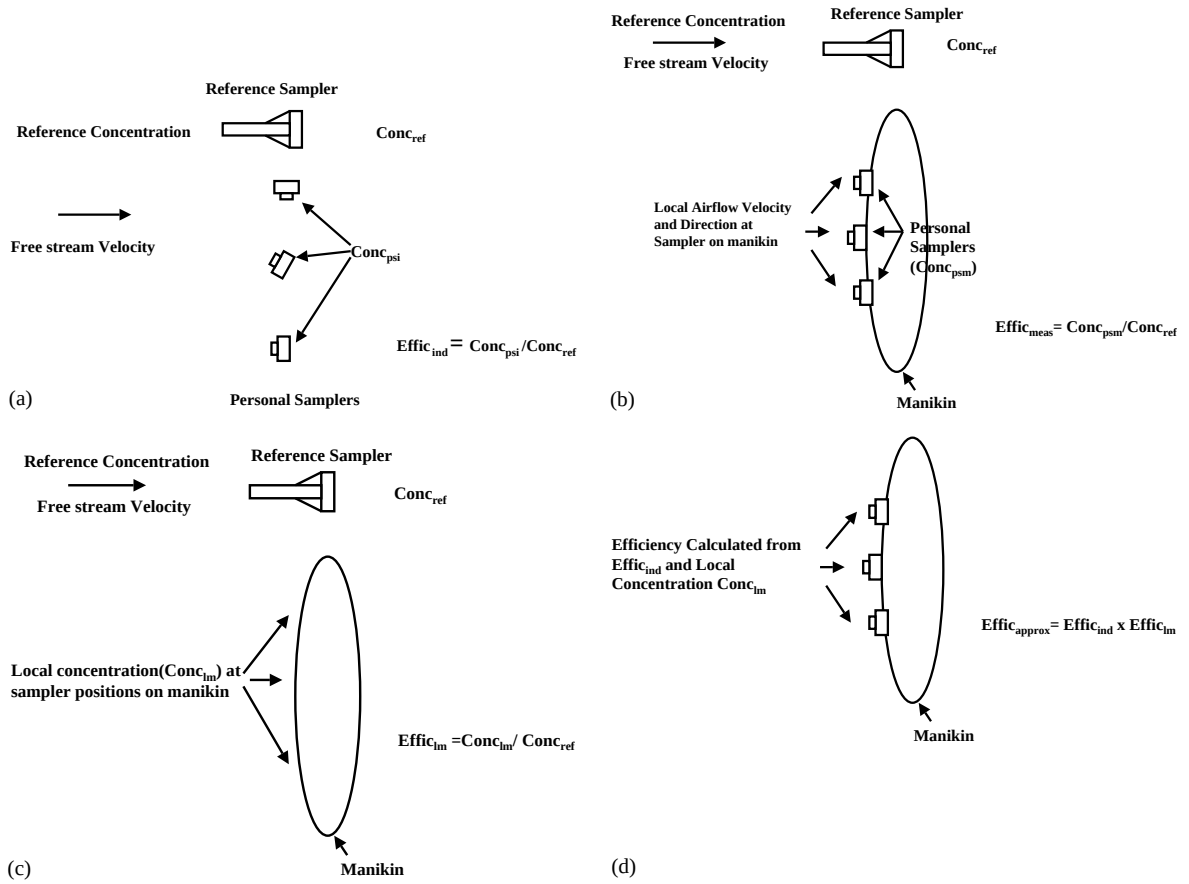

Fig. 4. (A) Sampling efficiency measured independent of manikin. (B) Measured sampling efficiency for manikin-mounted samplers. (C) Local manikin efficiency. (D) Approximated efficiency for manikin-mounted samplers.

This allows for the calculation of an approximated efficiency for manikin-mounted samplers, $\mathrm{Effic}_{\mathrm{approx}}$, using the independent efficiency and local-manikin concentration (Fig. 4D).

$$\mathrm{Effic}_{\mathrm{approx}} = (\mathrm{Effic}_{\mathrm{ind}})(\mathrm{Effic}_{\mathrm{lm}}). \tag{4}$$

If this relationship adequately describes the efficiency of manikin-mounted samplers then,

$$\mathrm{Effic}_{\mathrm{approx}} \approx \mathrm{Effic}_{\mathrm{meas}}. \tag{5}$$

It is important that the conditions used to determine $\mathrm{Effic}_{\mathrm{ind}}$ simulate the airflow conditions seen by the samplers when they are mounted on the manikin. The relevant value of $\mathrm{Effic}_{\mathrm{ind}}$ for a given sampler operating under particular sets of conditions needs to be selected. It is important to understand the airflow parameters experienced by samplers mounted on the manikin, as well as to have the ability to determine the local concentration at the inlets of manikin-mounted samplers.

3.2. Efficiency independent of the manikin

The GSP and IOM samplers were placed in the wind tunnel independent of the manikin. The samplers were operated at their commonly used sampling rates of 3.5 and 2 l/min, respectively. Their sampling efficiencies were determined in reference to the freestream isokinetic/isoaxial thin-walled reference samplers for wind speeds of 0.5, 1, and 2 m/s. These data were collected to create sampling performance curves for determination of sampling efficiency independent of the manikin. The samplers were oriented at 0°, 45°, and 90° angles to the freestream flow because these values covered the range of wind directions that the samplers had experienced while mounted on the manikin. Efficiency measurements were also made at a 0° orientation for wind speeds less than 0.5 m/s, by using the airflow created in the stagnation zone in front of a 0.29 m circular disk. These independent values of efficiency were applied to each of the three manikin orientations.

3.3. Local manikin concentration

From the air-velocity measurements and applicable regressions of the air-velocity data (described in Section 5), the specific locations, directions, and velocities of airflow were used to define isokinetic and isoaxial sampling conditions for determination of local-manikin concentration by near-body reference samplers. The inlets of the near-body reference samplers were carefully placed at exactly the proper location and orientation as dictated by the airflow data and were operated having inlet velocities equal to the resultant of the local velocity vectors measured with LDV.

3.4. Measured efficiency for manikin-mounted samplers

The GSP and IOM were then mounted on the manikin and operated using sampling rates of 3.5 and 2 l/min, respectively, which are the normal rates for occupational sampling. Their efficiencies were determined relative to isokinetic reference samplers operated at locations where flow disturbance due to the manikin was minimal or nonexistent as described earlier.

4. Results

4.1. Velocity measurements at a 0° angle, facing the wind

4.1.1. Chest area of manikin

At both the 0.5 and 2 m/s wind speeds, the velocity vectors of the airflow approaching the chest had the same relative direction, but their magnitudes differed accordingly (Fig. 5).

Overall, the air velocity at the center, right, and left positions was affected differently by the presence of the manikin. At the center position, as the wind approached the chest, the flow decelerated and approached a low average velocity having a slight upward component, while the direction remained pointed toward the manikin, forming a stagnation region that has been discussed previously (Rodes et al., 1995). At the positions 0.1 m to the left and 0.1 m to the right of the center, the velocity decreased less and changed direction for both wind speeds, but there was still a significant downstream (x direction) velocity component at positions close to the manikin for both the 0.5 and

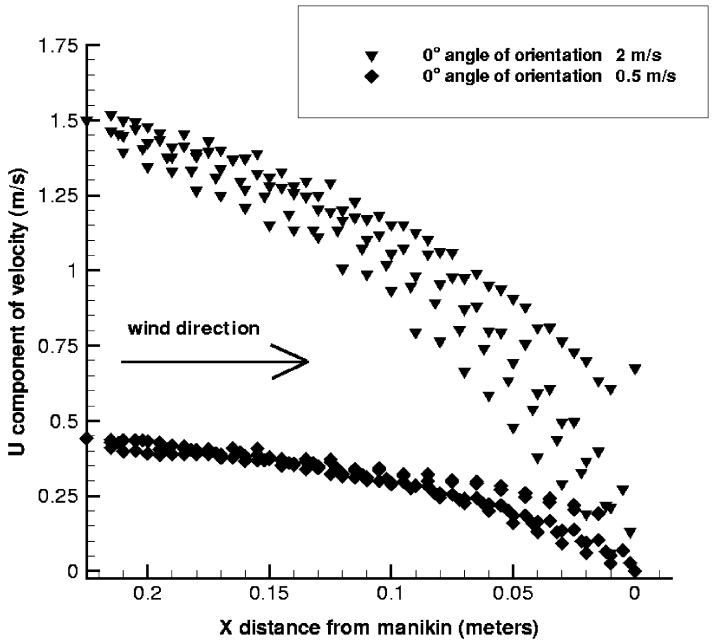

Fig. 5. Graphical representation of the U component of velocity for the manikin at a 0° angle of orientation for 0.5 and 2 m/s in the chest region of the manikin.

2 m/s wind speeds. The velocity profile was slightly different on the right and left of center positions, which is believed to be due to the unsymmetrical shape of the manikin. The zone of stagnation is visible in Fig. 5 as a noticeably decreasing velocity component at 0.1 m away from the surface of the manikin for the 2 m/s wind speed and at about 0.07 m for the 0.5 m/s wind speed.

If the GSP or IOM sampler were located in the center of the chest of the manikin, the flow approaching the inlet of each sampler would be different. Since the inlet of the GSP sampler is 0.075 m from the manikin the airflow would be parallel to the axis of the inlet and about 50% of the free stream flow while the airflow approaching the IOM would be only 20% of the free stream velocity because its inlet is only 0.03 m from the manikin. If either sampler were located 0.1 m to the right or left of center again the airflow seen by each sampler would be different. The flow approaching the inlet of the GSP would be approximately parallel to the axis of the inlet and 50% of the freestream while that approaching the IOM would be 50% of freestream but at an angle of about 45° to axis of inlet.

4.1.2. Face area

Airflow behavior around the face area was similar for both the 0.5 and 2 m/s wind speeds, and decelerated somewhat as it approached the head. This observed deceleration was not as significant as in the chest area of the manikin; the flow was not $< 50\%$ of the external wind at any location studied but was somewhat unsymmetrical on the right or left of center because the manikin's head was turned slightly to the left.

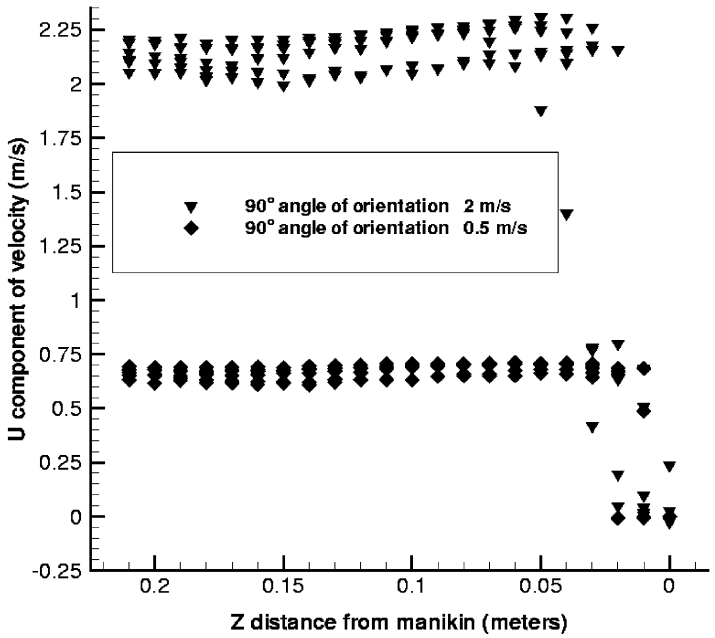

Fig. 6. Graphical representation of the U component of velocity for the manikin at a 90° angle of orientation for 0.5 and 2 m/s for distances ranging from 0.2 to 0.05 m from the center of the chest.

4.2. *Measurements made with manikin at a* 90° *angle to the wind*

4.2.1. *Chest area*

For the 2 m/s wind speed, there was a slight acceleration of the flow at decreasing distances from the chest and little change of direction up to about 0.05 m from the surface where the velocity dropped off drastically and turbulence increased. At the 0.5 m/s wind speed, there was little change in air velocity or direction until about 0.01 m from the surface (Fig. 6). For the 2 m/s wind speed, there was indication of turbulence observed at further distances from the surface than for 0.5 m/s. Generally flow turbulence did not appear to occur until very close to the surface at the upwind position of the manikin; however, as the air passed the manikin, the velocity fluctuations increased over a larger area downstream. The measurements on the back of the manikin oriented at 90° to the wind were similar to those on the chest side with a slight acceleration of the flow on approach and some turbulence disruption closer to the surface. Figs. 6 and 7 show the velocity components in the chest area of the manikin for heights of 0.41 and 0.38 m. The observed zone of separation is visible in Fig. 6 as a drastic drop off in velocity that occurs just inside of 0.05 m for both the 0.5 and 2 m/s wind speeds.

4.2.2. *Face area*

The airflow passing the face area of the manikin when it was at a 90° angle to the wind showed a pattern similar to that at the chest. The flow experienced a slight acceleration of about 15% at a distance of 0.05 m from the surface. The flow became somewhat turbulent closer to the surface,

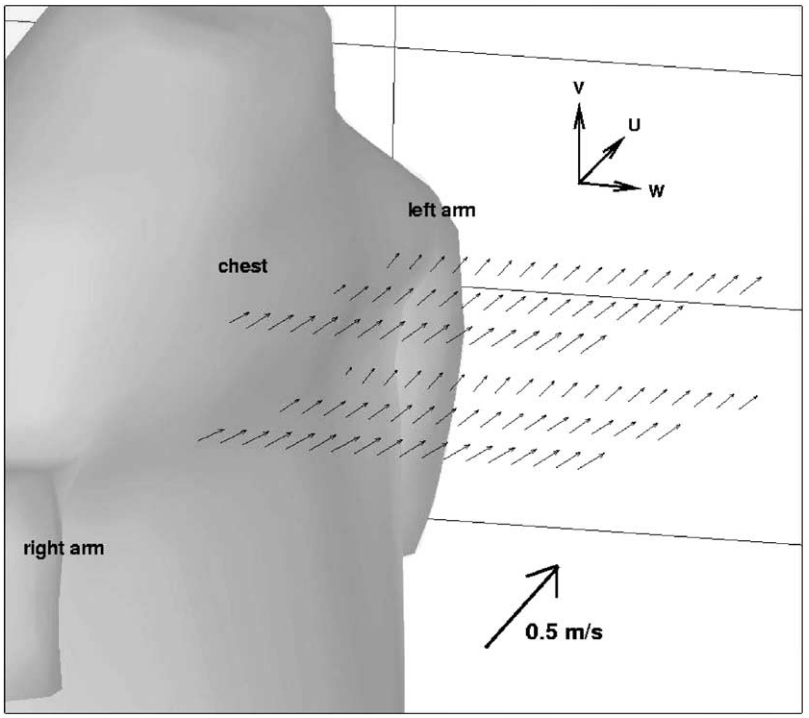

Fig. 7. Velocity vectors when the manikin orientation is at a 90° angle of orientation for 0.5 m/s wind speed. The data shown are for two heights (0.43 and 0.38 m) and left, center, and right of chest.

and had a lower intensity than freestream flow. The disrupted flow also extended further from the manikin at the higher wind speed, and it appeared that the flow was disrupted further from the manikin in the center than at the upstream (right) position. However, at the downwind position there was less disruption probably because at this point the turbulence was already dissipating.

4.3. Measurements made with manikin at 180° angle to the wind

The airflow downstream of the manikin was turbulent, and the relative standard deviation of the mean velocity was typically 100% or above. A two-dimensional graphical representation (Fig. 8) indicates that there are no easily observable trends of the data. Therefore, the data are not currently eligible for modeling and can only be used for looking up values of interest from the data set.

4.3.1. Chest

For the 0.5 m/s wind speed, most velocities were very low near the surface, having the lowest average velocity at the center of the manikin. At the 2 m/s wind speed, there was a large lateral component of the velocity near the manikin at some positions. At the 0.5 m/s windspeed, the maximum wind speed near the manikin was not more than 0.2 m/s at most measurement points.

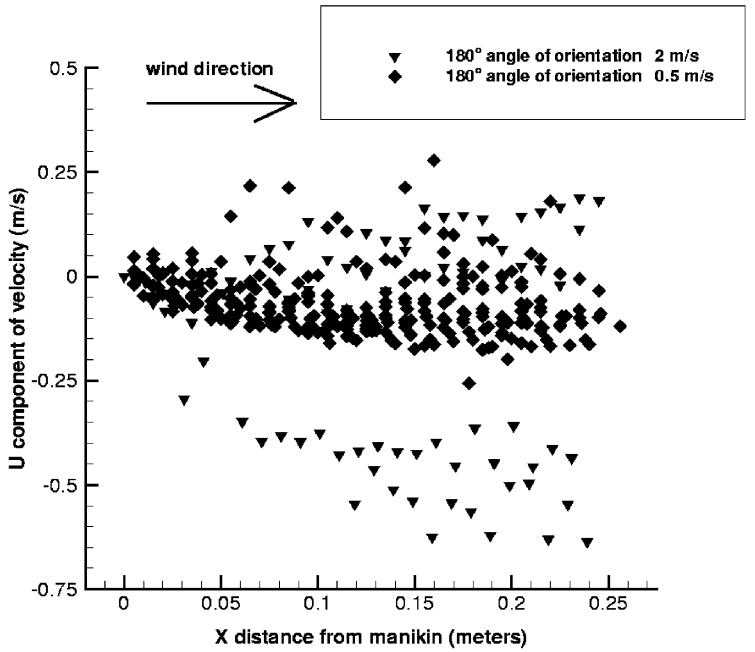

Fig. 8. Graphical representation of the U component of velocity for the manikin at a 180° angle of orientation for 0.5 and 2 m/s for the 0.43 and 0.38 m above floor of wind tunnel and left, center, and right of chest.

4.3.2. Face area

For the flow around the back of the head, the velocity was low, especially in the center of the breathing zone at 0.5 m/s. At the 2 m/s wind speed, there was a higher lateral component to the velocity near the face area.

5. Analysis of flow field around manikin

Data collected for the flow fields were extensive; therefore, regression models of the data were developed for a range of locations, so that the data could be effectively presented in this paper and more easily used at a later time. The data represent an accessible resource for comparison or use in future experiments.

Data consisted of means and standard deviations of velocity components. Due to the nature of data collection, measurement of steady flow about the mean, the time-dependent values making up the mean of the velocity components, were not retained. There was concern the variance about a mean at a sampled location would differ from location to location. Therefore, to decide whether regressing the mean values was appropriate, we ran tests for homogeneity of variance using the modified-Levene test, which were conducted to measure variance constancy from mean to mean (Neter, Kunter, Nachtsheim, & Wasserman, 1996). This technique is a test on the t-distribution for variance of means with risk, in this case, controlled at $\alpha = 0.05$.

Table 1
Regression models for the full-size manikin at a 0° angle of orientation (manikin facing the wind)

Location	Coordinates (m) see Fig. 1	Freestream velocity (m/s)	Regression models for velocity U, V, W (see Fig. 1) components	R^2	%CV
Chest	$x = 0.225$–0.005	2	$U = LN(1.445 + 14.39x - 1.104z)$	0.952	6.88
	$y = 0.43$		$V = LN(1.534 - 1.707x - 0.510z)$	0.650	6.23
	$z = -0.1, 0, 0.1$		$W = LN(1.086 - 0.344x + 3.767z)$	0.746	17.33
Chest	$x = 0.225$–0.005	2	$U = LN(1.357 + 14.10x - 1.57z)$	0.918	9.11
	$y = 0.38$		$V = LN(1.534 - 1.707x - 0.510z)$	0.650	6.23
	$z = -0.1, 0, 0.1$		$W = LN(1.086 - 0.344x + 3.767z)$	0.746	17.33
Chest	$x = 0.225$–0.005	0.5	$U = LN(1.138 + 2.0x - 0.289z)$	0.930	2.65
	$y = 0.43$		$V = LN(0.798 - 0.205x + 0.788y - 0.142z)$	0.633	1.792
	$z = -0.1, 0, 0.1$		$W = LN(0.993 + 0.149x + 1.065z)$	0.825	3.98
Chest	$x = 0.225$–0.005	0.5	$U = LN(1.12 + 2.10x - 0.266z)$	0.919	2.87
	$y = 0.38$		$V = LN(1.081 - 0.061x - 0.134z)$	0.594	0.878
	$z = -0.1, 0, 0.1$		$W = LN(0.985 + 0.224x + 1.014z)$	0.80	4.15
Face area	$x = 0.245$–0.008	2	$U = LN(1.118 + 12.43x + 2.993y - 5.775z)$	0.904	6.478
	$y = 0.58, 0.63$		$V = LN(4.582 + 0.067x - 5.443y - 0.994z)$	0.720	15.05
	$z = -0.05, 0, 0.06$		$W = LN(1.231 + 0.518x - 0.431y + 3.356z)$	0.488	15.12
Face area	$x = 0.245$–0.008	0.5	$U = LN(1.536 + 1.081x - 0.345y - 0.877z)$	0.827	2.509
	$y = 0.58, 0.63$		$V = LN(0.973 + 0.048x + 0.199y - 0.311z)$	0.432	1.562
	$z = -0.05, 0, 0.06$		$W = LN(1.081 + 0.216x - 0.172y + 0.897z)$	0.538	3.936

Note: Regressions are valid only for ranges listedin the second column.

The modified-Levene tests on the velocimetry data indicated that variance was not different among laser-Doppler measurements. There were several isolated incidences of modified-Levene test failures, which were limited to the V or W component of velocity and, thus, had little impact on the resultant velocity vectors or regression models.

Graphical analysis showed that much of the data behaved exponentially; therefore, log transformations were conducted on the data sets prior to regression. Regression models were created using the statistical analysis package, SAS 6.12 (Sas Institute Inc., Cary, NC, USA). As a first try, predictor variables consisted of each Cartesian coordinate; however, it became clear that the primary distance from the manikin was the most effective regressor.

Table 1 shows the regression equations that can be used to predict velocity at a range of locations near the manikin, facing the wind. From these equations one can predict the velocity at positions in front of the manikin, defined by x, y, and z coordinates, but only in the range where the model is appropriate, where x is the distance from the manikin, y is the height above the wind tunnel floor, and z is the position right and left of center. Appropriate ranges for respective models are given in the second column of the table.

6. Sampling efficiency measurements

6.1. Sampling efficiency independent of manikin

Figs. 9 and 10 show the sampling efficiency of the IOM and GSP samplers in free air, for wind speeds of 0.5, 1, and 2 m/s, and when mounted on a disk, for wind speeds less than 0.5 m/s.

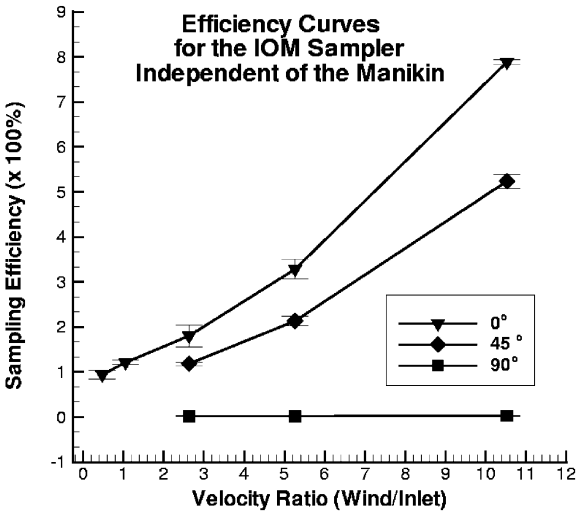

Fig. 9. Sampling efficiency of IOM personal sampler measured independently of the manikin. Orientations include 0°, 45°, and 90°.

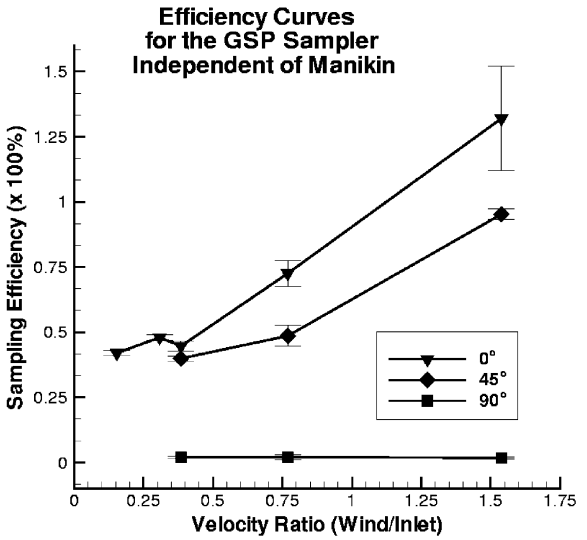

Fig. 10. Sampling efficiency of GSP personal sampler measured independently of the manikin. Orientations include 0°, 45°, and 90°.

Each sampler was tested at 0°, 45° and 90° angles to the wind in free air, but only at 0° for the samplers on the disk. The data are plotted as efficiency versus the ratio of wind to inlet velocity for each type of sampler because the data were used in this form for calculating the efficiency of samplers independent of the manikin. The data taken by the samplers mounted on the disk match up reasonably well with those taken in free air and show that the sampling efficiencies tend to approach approximately 1 for IOM and 0.45 for GSP, as the velocity ratio is decreased. This agrees with

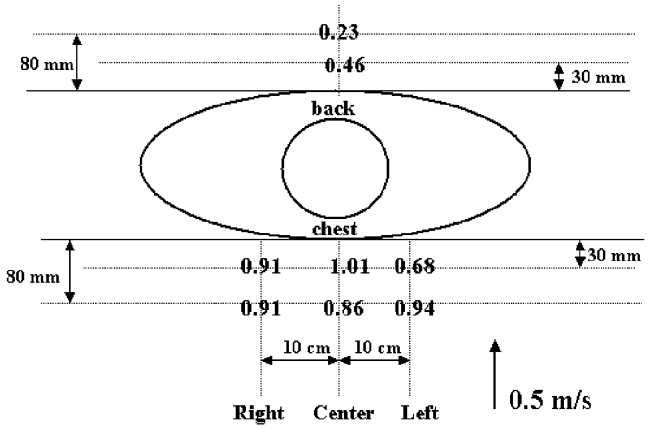

Fig. 11. Local-manikin efficiencies around full-sized manikin at an orientation of 0° and experiencing a wind speed of 0.5 m/s.

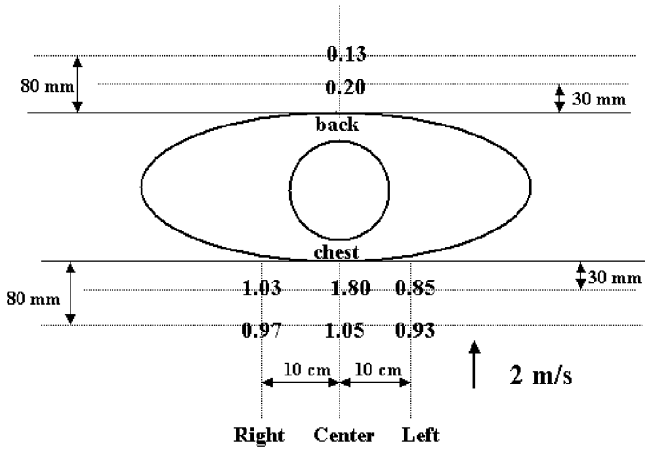

Fig. 12. Local-manikin efficiencies around full-sized manikin at an orientation of 0° and experiencing a wind speed of 2 m/s.

previous data taken in still air (Kenny et al., 1999) where an efficiency of about 0.8 was measured for the IOM sampler and 0.4 for the GSP sampler for 70 μm particles.

6.2. Local-manikin efficiency

Local-manikin efficiency was determined for manikin orientations of 0°, 90°, and 180° angles to the wind at windspeeds of 0.5 and 2 m/s. Figs. 11 and 12 show the measured local-manikin efficiencies in front and back of the manikin when it was facing the wind. In the front of the manikin, at the

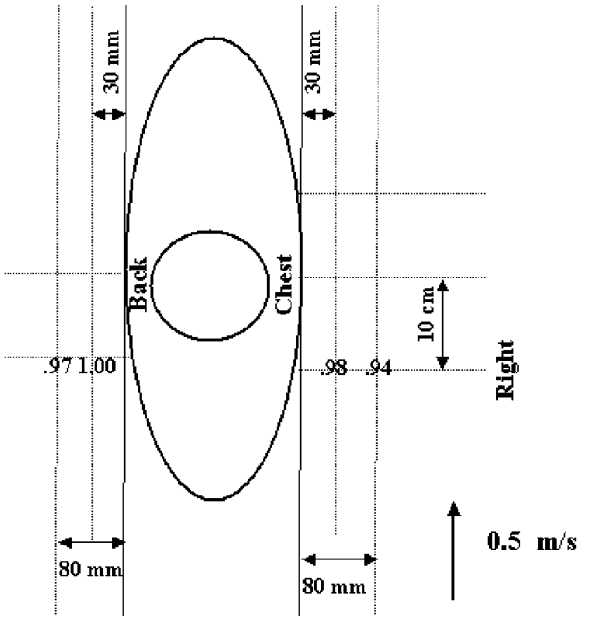

Fig. 13. Local-manikin efficiencies around full-sized manikin at an orientation of 90° and wind speed of 0.5 m/s.

windspeed of 0.5 m/s, and a distance of 0.03 m from the surface, the local-manikin concentration was similar to the reference concentration. At the 2 m/s wind speed, the center of the manikin had a higher local concentration, especially at a location of 0.03 m from the manikin where the local concentration was about 1.8 times the reference concentration. The back of the manikin (180° to the wind) showed lower local concentrations than the reference concentration. At 0.5 m/s the local concentration was 0.46 and 0.23 times the reference concentration at 0.03 and 0.08 m, respectively. At 2 m/s the local concentration was even lower, 0.20 and 0.13 times the reference concentration. For the 0° orientation the relative standard deviation (RSD) of the concentration measurements varied from 2% to 8% for the different positions. At the 180° orientation the RSD of the measurements was higher (9–21% for the different positions), but this may be due to the lower efficiency. Figs. 13 and 14 show the measured local-manikin efficiencies when the manikin was at 90° to the wind, at wind speeds of 0.5 and 2 m/s, respectively. At the distance of 30 and 80 mm from the manikin, the measured local-manikin concentration was approximately the same as the reference concentration at both the 0.5 and 2 m/s wind speed. The RSD for these measurements varied from 1–10% at the different positions.

There was a noticeable change in local-manikin concentration between the two measurement distances of 0.08 and 0.03 m. When averaged, for data collected at a specific location, the difference between the two distances was low in some cases and higher in others. Table 2 shows the average percent change from the 0.08 m location to the 0.03 m location. Average concentration increased in all cases, except for the manikin oriented at 0° experiencing a wind speed of 0.5 m/s. However, for the center positions oriented at 0°, both the 0.5 and 2 m/s wind speeds showed an increase from 0.08 to 0.03 m locations: changes of 15% and 42%, respectively.

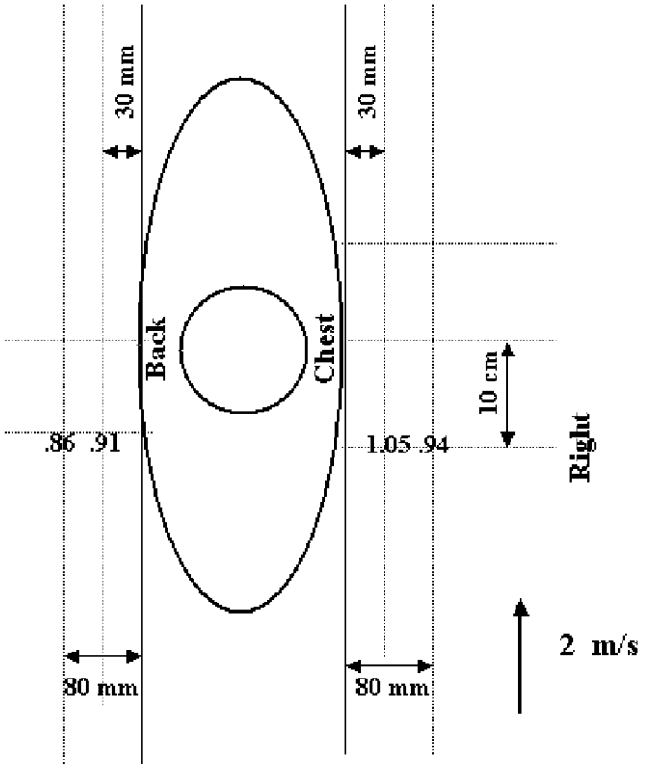

Fig. 14. Local-manikin efficiencies around full-sized manikin at an orientation of 90° and wind speed of 2 m/s.

Table 2
Average percent change in local-manikin concentration from the 0.08 m location to the 0.03 m location for the 0°, 90° and 180° orientations and for 0.5 and 2 m/s wind speeds

Windspeed (m/s)	Manikin orientation		
	0°	90°	180°
0.5	3.7	4	50
2	20.3	8.2	35

6.3. Approximation of sampling efficiency for manikin-mounted samplers and comparison with measured efficiencies

Tables 3 and 4 compare the approximated and measured efficiencies for IOM samplers mounted on the manikin at wind speeds of 0.5 and 2 m/s. At 0.5 m/s when the manikin faced the wind (0° orientation, with the manikin-mounted sampler experiencing a 45° airflow direction), both the approximated and measured efficiencies were close to unity, and there was little variation due to position on the manikin. There was uncertainty in the approximated efficiency for this

Table 3
Approximated and measured sampling efficiency of the IOM inhalable sampler, 0.5 m/s freestream air velocity

Position $R = 0.1$ m right $C =$ center $L = 0.1$ m left	[b]Wind velocity-inlet (m/s)	Velocity ratio (wind/inlet)	[c]Angle of airflow	Local manikin effic. ($effic_{lm}$) (Eq. (3); Figs. 10 and 12)	Ind. effic. ($effic_{ind}$) (Eq. (1); Fig. 8)	Approx effic. ($effic_{approx}$) (Eq. (4))	Measured effic. ($effic_{meas}$) (Eq. (2)) RSD in ()	% Error Meas-approx/Meas $\times 100\%$
[a]Angle to wind = 0								
R	0.21	1.1	45	0.91	1	0.91	0.87(0.04)	4.6
C	0.10	0.53	45	1.01	1	1.01	0.94(0.05)	7.5
L	0.30	1.6	45	0.68	1.4	0.95	1.03(0.06)	7.8
[a]Angle to wind = 180								
C	0.10	0.53	0	0.46	1	0.46	0.49(0.08)	6.1
[a]Angle to wind = 90								
R	0.6	3.2	90	0.99	0.02	0.02	0.05(0.01)	60
R/*C*/*L*	0.6	3.2	90	0.99	0.02	0.02	0.18(0.12)	89

[a]Angle of external airflow with respect to manikin.
[b]Wind velocity approaching inlet of manikin-mounted sampler.
[c]Angle of airflow with respect to inlet of manikin-mounted sampler.

location because the independent efficiency was determined from the extension of the curve at 0°, as no data were available for 45°, at this low wind speed. However the curves for 0°, and 45°, behaved similarly at lower velocity ratios, and, therefore, this extrapolation was felt justified.

At 180°, the local concentration was found to be lower than the reference. The independent efficiency was assumed to be unity due to the low wind speed, and approximated efficiency was in agreement with the measured efficiency. At 90° there was more variation in the measured efficiency data than at the other orientations but both approximated and measured efficiencies were low.

For the IOM sampler at the 2 m/s windspeed and the manikin facing the wind, the approximated and measured efficiencies had greater variability from location to location, and the center position had the highest efficiency. In the center position, the independent efficiency of the IOM sampler was lower, while the relative concentration was higher, resulting in a higher approximated sampler efficiency, which agreed with the measured efficiency. However, at the right and left positions, the independent efficiency of the sampler was higher while the local concentration was lower, resulting in an approximated efficiency that was comparable to the center position. For sampling on the chest when the manikin's back was to the wind (180° orientation), there was good agreement between approximated efficiency and measured efficiencies, assuming the sampler collected with an efficiency of 1 at the reduced concentration present there. When the manikin was at 90° to the wind, again the measured efficiencies were low and variable.

Table 4
Approximated and measured sampling efficiency of the IOM inhalable sampler, 2 m/s external freestream velocity

Position $R = 0.1$ m right $C =$ center $L = 0.1$ m left	[b]Wind velocity-inlet (m/s)	Velocity ratio (wind/inlet)	[c]Angle of airflow	Local manikin effic. ($effic_{lm}$) (Eq. (3); Figs. 11 and 13)	Ind. eff. ($effic_{ind}$) (Eq. (1); Fig. 8)	Approx eff. ($effic_{approx}$) (Eq. (4))	Measured eff. ($effic_{meas}$) (Eq. (2)) RSD in ()	% Error Meas-approx/Meas $\times 100\%$
[a]Angle to wind = 0								
R	0.77	4.11	45	1.03	1.6	1.6	2.22(0.27)	28
C	0.53	2.8	45	1.8	1.2	2.2	2.53(0.24)	13
L	1.06	5.61	45	0.85	2.2	1.9	1.87(0.30)	1.6
[a]Angle to wind = 180								
C	0.45	2.4	0	0.20	1.2	0.24	0.27(0.08)	11
[a]Angle to wind = 90								
$R/C/L$	2.3	12.1	90	0.93	0.02	0.02	0.06(0.02)	67

[a]Angle of external airflow with respect to manikin.
[b]Wind velocity approaching inlet of manikin-mounted sampler.
[c]Angle of airflow with respect to inlet of manikin-mounted sampler.

Tables 5 and 6 show the approximated and measured efficiencies of the GSP sampler while mounted on the manikin. At 0.5 m/s and the manikin facing the wind, both the approximated and measured efficiencies are close to 0.4 and are uniform from position to position. At 180° to the wind, the approximated efficiency agrees well with the measured efficiency only by assuming the independent efficiency is 1. This assumption is not justified based on Fig. 9 and the complex turbulent nature of the flow with the manikin at 180° does not allow easy interpretation. Turbulence is known to affect sampling efficiency (Vincent, Emmett, & Mark, 1985; Wiener, Okazaki, & Willeke, 1988).

At the 90° orientation, the approximated and measured efficiencies are both $< 5\%$. For the GSP sampler at 2 m/s when the manikin faced the wind, the approximated efficiency is slightly higher (0.7) than the measured efficiency (0.6), and this difference is relatively constant for the various positions where samplers were placed. At 180° to the wind, the approximated and measured efficiencies have good agreement only if the independent efficiency is assumed to be 1 and again this assumption is not justified based on Fig. 9. At 90° to the wind, the calculated and measured efficiencies are again both $< 5\%$.

7. Discussion

The work presented in this paper is the result of a study to determine the effect airflow behavior has on the sampling efficiency of manikin-mounted samplers. In the first part of the study, measurements of airflow velocity and direction were made with LDV. These measurements defined the location,

Table 5
Approximated and measured sampling efficiency of the GSP inhalable sampler, 0.5 m/s external freestream velocity

Position $R = 0.1$ m right $C =$ center $L = 0.1$ m left	[b]Wind velocity-inlet (m/s)	Velocity ratio (wind/inlet)	[c]Angle of airflow	Local manikin effic. ($effic_{lm}$) (Eq. (3); Figs. 10 and 12)	Ind. eff. ($effic_{ind}$) (Eq. (1); Fig. 9)	Approx eff. ($effic_{approx}$) (Eq. (4))	Measured eff. ($effic_{meas}$) (Eq. (2)) RSD in () ()	% Error Meas-approx/Meas $\times 100\%$
[a]Angle to wind = 0								
R	0.31	0.24	0	0.91	0.45	0.41	0.40(0.02)	2.5
C	0.25	0.19	0	0.86	0.45	0.39	0.45(0.02)	2.7
L	0.33	0.26	0	0.94	0.45	0.42	0.43(0.05)	2.3
[a]Angle to wind = 180								
C	0.1	0.076	0	0.23	1	0.23	0.27(0.05)	14.8
[a]Angle to wind = 90								
L	0.6	0.45	90	0.96	0.02	0.02	0.05(0.01)	60

[a]Angle of external airflow with respect to manikin.
[b]Wind velocity approaching inlet of manikin-mounted sampler.
[c]Angle of airflow with respect to inlet of manikin-mounted sampler.

orientation, and inlet velocity of near-body reference samplers that were used to determine the aerosol concentration in the near-body region of a manikin.

This work has shown a measurable difference in aerosol concentration at the distances of 0.08 and 0.03 m away from the manikin for orientations of 0°, 90°, and 180°. These differences in concentration at different distances from the manikin affected the GSP and IOM samplers differently due to their inlet lengths. The efficiencies of these two samplers are significantly dissimilar—up to 300%—at the three manikin orientations studied.

A primary goal of the study was an attempt to gain more insight into the characteristics of sampling efficiency of two inhalable dust samplers for development of a method to simplify the testing of air samplers. A technique was developed to approximate sampling efficiency for near-body sampling, based on the adjustment of sampling efficiency determined independently of a manikin, using the local-manikin concentration at the proposed location of the sampler of interest.

This technique resulted in data that agreed with measured sampling efficiency for the IOM and GSP samplers at orientations of 0° and to a lesser extent with measured sampling efficiency for both samplers at the 90°, orientation. This finding suggests the detailed shape of a full-sized manikin may not be as significant an influence on airflow behavior as the formation of stagnation and separation zones at the 0° and 90° orientations. However, the gross shape of the full-sized manikin very likely governs the depth and size of the zones of stagnation and separation. Therefore, a bluff-body shape used for sampling-efficiency determination of samplers, having different inlet lengths, should be somewhat similar to the chest area of a full-sized manikin and have the characteristics of being

Table 6
Approximated and measured sampling efficiency of the GSP inhalable sampler, 2 m/s external freestream velocity

Position $R = 0.1$ m right $C =$ center $L = 0.1$ m left	[b]Wind velocity-inlet (m/s)	Velocity ratio (wind/inlet)	[c]Angle of airflow	Local manikin effic. ($effic_{lm}$) (Eq. (3); Figs. 11 and 13)	Ind. eff. ($effic_{ind}$) (Eq. (1); Fig. 9)	Approx eff. ($effic_{approx}$) (Eq. (4))	Measured eff. ($effic_{meas}$) (Eq. (2)) RSD in () ()	% Error Meas-approx/Meas $\times 100\%$
[a]Angle to wind = 0								
R	1.1	0.85	0	0.97	0.8	0.77	0.60(0.04)	23
C	0.88	0.68	0	1.05	0.64	0.67	0.71(0.16)	5.6
L	1.2	0.92	0	0.93	0.85	0.79	0.64(0.08)	23.4
[a]Angle to wind = 180								
C	0.4	0.30	0	0.13	1	0.13	0.10(0.03)	30
[a]Angle to wind = 90								
L	2.3	1.74	90	0.96	0.02	0.02	0.04(0.01)	50

[a]Angle of external airflow with respect to manikin.
[b]Wind velocity approaching inlet of manikin-mounted sampler.
[c]Angle of airflow with respect to inlet of manikin-mounted sampler.

wider than thick, as well as rounded on the edges, i.e., an elliptically shaped cylinder, to be consistent with the technique presented here.

It is interesting to note that the samplers studied in this work (IOM and GSP) have inlets in regions of different flow. The IOM has its inlet at 20–30 mm from the manikin surface and would be in the stagnation region if mounted in the center of chest, but the inlet of the GSP, which is 70–80 mm from the manikin surface, would be just at the boundary of the stagnation region. If these samplers were mounted right or left of center, the IOM would be in a region having a large lateral component to the flow, while the flow would be almost straight into the GSP at this position on the manikin. As a result, the GSP inlet is exposed to flow that better approximates that of the breathing zone when the manikin faces the wind. The situation becomes more complicated when the manikin is at a 90° angle to the wind. At distances greater than 50 mm from the chest or breathing zones, the flow is perpendicular to the chest and face. At closer approach there is increased velocity fluctuation, especially at higher wind speeds and positions further downstream. The inlet of the GSP would be outside these more turbulent regions, but the IOM could be in them depending on where it was mounted on the chest of the manikin, as well as what the value of the wind speed was. The breathing zone also showed some regions of turbulent flow at higher wind speeds and downwind positions. When the manikin is at a 180° angle to the wind, both the face area and inlets to IOM and GSP samplers mounted on the chest are located in regions of low flows, and the maximum velocity expected to be seen by the samplers and the breathing zone is near zero at the 0.5 m/s wind speed. Because of the nature of this flow and the measurement technique used, only a general

description can be made, and further study might result in a more detailed analysis of the flow under these conditions. The flow approaching the manikin at 180° needs more study due to its turbulent nature. In this study only average flows were used in predicting efficiency but the situation is more complicated. No presently available model can be used to adequately describe efficiency. In this study it was assumed that the flow was low and both samplers had an efficiency of 1. Perhaps this efficiency can be justified for IOM sampler which is closer to the manikin where the velocity is uniformly low (Fig. 8) but not for GSP sampling (Fig. 9).

Knowing which airflow patterns approach the manikin should allow for better understanding of the parameters that affect the sampling efficiency of manikin-mounted samplers and might allow for different testing procedures and development of performance specifications for inhalable dust samplers. The proposed testing procedures would involve analysis of the samplers independently of the manikin under well-defined conditions. This has been addressed for the manikin in still air (Kenny et al., 1999) where it was found that samplers tested off the manikin gave similar results to manikin-mounted samplers. For the manikin at higher wind speeds, the samplers should be tested under defined conditions of airflow that would simulate those of manikin-mounted samplers at a given external wind speed. This information could then be combined with knowledge of how the concentration varied around the manikin to define the test conditions.

Performance criteria for these samplers would then be developed by specifying how samplers would perform in these well-defined airflows. Such application could be applied by looking at inhalability criteria as a function of windspeed, wind direction, and particle size. This would provide better guidance in the development of samplers to the present methods of testing samplers while mounted on a manikin under direction-averaged conditions which do not define how samplers perform at specified airflows.

Further work in this area would include verification of the results of this study at more particle sizes. Limited resources and time did not allow more than one particle size to be studied in this work. Better understanding of the functioning of samplers in turbulent flow (such as that encountered with the manikin at 180° to the wind) would help to gain insight into the performance of samplers under these conditions.

Empirical experiments designed to expand the knowledge of the airflow characteristics at the inlets of manikin-mounted samplers are time consuming, difficult, and expensive. Therefore, future work may be better accomplished by using simplified, but accurate testing techniques, as well as computational modeling of airflow and particle behavior in gaining even greater understanding of personal air samplers.

Acknowledgements

The authors are indebted to Drs. Paul Baron, Teh-Hsun Chen, Karl Snyder, Sid Soderholm, and Robert Konecny at NIOSH for their critiques and advice during the experiments, analysis, and manuscript preparation. In addition the authors would like to thank Drs. Doug Landsittel and Andrew Maynard, Mr. Kurt Brumbaugh, and Anne Votaw also of NIOSH, for their constructive critiques and editorial comments of the prepared manuscript. In addition, the authors would like to thank Dr. Wafik Iskander of West Virginia University for his statistical guidance in analysis of the LDV data.

References

Aitken, R. J., Baldwin, P. E. J., Beaumont, G. C., Kenny, L. C., & Maynard, A. D. (1999). Aerosol inhalability in low air movement environments. *Journal of Aerosol Science*, *30*, 199–219.

Baldwin, P. E. J., & Maynard, A. (1998). A survey of wind speeds in indoor workplaces. *Annals of Occupational Hygiene*, *42*, 303–313.

Botham, R. A., Hughson, G. W., Vincent, J. H., & Mark, D. (1991). The development of a test system for investigating the performances of personal aerosol samplers under actual workplace conditions. *American Industrial Hygiene Association, Journal*, *52*, 423–427.

Buchan, R. M., Soderholm, S. C., & Tillery, M. I. (1986). Aerosol sampling efficiency of 37-mm filter cassettes. *American Industrial Hygiene Association, Journal*, *47*, 825–831.

Chung, I., & Dunn-Rankin, D. (1997). Experimental investigation of air flow around blunt aerosol samplers. *Journal of Aerosol Science*, *28*, 289–305.

Chung, K. Y. K., Ogden, T. L., & Vaughan, N. P. (1987). Wind effects on personal dust samplers. *Journal of Aerosol Science*, *18*, 159–174.

Dunnett, S. J. (1997). A numerical study of the flow field in the vicinity of a bluff body with aspiration oriented to the flow. *Atmospheric Environment*, *31*, 3745–3752.

Dunnett, S. J. (1999). An analytical investigation into the nature of the airflow near a spherical bluff body with suction. *Journal of Aerosol Science*, *30*, 163–171.

Dunnett, S. J., & Vincent, J. H. (2000). A mathetmatical study of aerosol sampling by an idealized blunt sampler oriented at an angle to the wind: role of gravity *Journal of Aerosol Science*, *31*, 1187–1203.

Flynn, M. R., Chen, M., Kim, T., & Muthedath, P. (1995). Computational simulation of worker exposure using a particle trajectory method. *Annals of Occupational Hygiene*, *39*, 277–289.

Flynn, M. R., & Ljungqvist, B. (1995). A review of wake effects on worker exposure. *Annals of Occupational Hygiene*, *39*, 211–221.

Hinds, W., & Kuo, T. (1995). A low velocity wind tunnel to evaluate inhalability and sampler performance for large dust particles. *Applied Occupational and Environmental Hygiene*, *10*, 549–556.

Hinds, W., Tatyan, K., & Kennedy, N. J. (2001). Comparison of a simplified and full-size mannequin for the evaluation of inhalable sampler performance. *Aerosol Science and Technology*, *35*, 214–220.

Johnson, A. E., Fletcher, B., & Saunders, C. J. (1996). Air movement around a worker in a low-speed field. *Annals of Occupational Hygiene*, *40*, 57–64.

Kenny, L. C., Aitken, R. J., Baldwin, P. E. J., Beaumont, G. C., & Maynard, A. D. (1999). The sampling efficiency of personal inhalable aerosol samplers in low air movement environments. *Journal of Aerosol Science*, *30*, 627–638.

Kenny, L. C., Aitken, R. J., Chalmers, C., Fabries, J. F., Gonzalez-Fernandez, E., Kromhout, H., Liden, G., Mark, D., Riediger, G., & Prodi, V. (1997). A collaborative European study of personal inhalable aerosol sampler performance. *Annals of Occupational Hygiene*, *41*, 135–153.

Kim, T., & Flynn, M. R. (1991). Airflow pattern around a worker in a uniform freestream. *American Industrial Hygiene Association, Journal*, *52*, 287–296.

Li, S., Lundgren, D. A., & Rovell-Rixx, D. (2000). Evaluation of six inhalable aerosol samplers. *American Industrial Hygiene Association, Journal*, *61*, 506–516.

Liden, G., Juringe, L., & Gudmundsson, A. (2000). Workplace validation of a laboratory evaluation test of samplers for inhalable and total dust. *Journal of Aerosol Science*, *31*, 199–219.

Mark, D., & Vincent, J. H. (1986). A new personal samplers for airborne total dust in workplaces. *Annals of Occupational Hygiene*, *30*, 89–102.

Mark, D., Vincent, J. H., & Witherspoon, W. (1985). Applications of closely graded powders of fused alumina as test dust for aerosol studies. *Journal of Aerosol Science*, *16*, 125–131.

Neter, J., Kutner, M. H., Nachtsheim, C. J., & Wasserman, W. (1996). *Applied linear regression models* (3rd ed.) (pp. 112–114).

Rodes, C. E., Kamens, R. M., & Wiener, R. W. (1995). Experimental consideration for the study of contaminant dispersal near the body. *American Industrial Hygiene Association, Journal*, *56*, 535–545.

Smith, J. P., Bartley, D. L., & Kennedy, E. R. (1998). Laboratory investigation of the mass stability of sampling cassettes from inhalable aerosol samplers. *American Industrial Hygiene Association, Journal*, *59*, 582–585.

Smith, J. P., Bartley, D., & Watkins, D. (1999). Development of a large particle aerosol distribution system for testing manikin-mounted samplers. *Aerosol Science and Technology*, *30*, 454–466.

Tatum, V. L., Ray, A. E., & Rovell-Rixx, D. S. (2001). The performance of personal inhalable dust samplers in wood-products industry facilities. *Applied Occupational and Environmental Hygiene*, *16*, 763–769.

Tsai, P. J., Vincent, J. H., & Mark, D. (1996). Semi-empirical model for the aspiration efficiencies of personal aerosol samplers of the type widely used in occupational hygiene. *Annals of Occupational Hygiene*, *40*, 93–113.

Vincent, J. H., Emmett, P. C., & Mark, D. (1985). The effects of turbulence on the entry of airborne particles into a blunt dust sampler. *Aerosol Science and Technology*, *4*, 17–29.

Wen, X., & Ingham, D. B. (2000). Aspiration efficiency of thin-walled cylindrical aerosol sampler at yaw orientations with respect to the wind. *Journal of Aerosol Science*, *31*, 1355–1365.

Wiener, R. W., Okazaki, K., & Willeke, K. (1988). Influence of turbulence on aerosol sampling efficiency. *Atmospheric Environment*, *22*, 917–928.

Wood, J. D., & Birkett, J. L. (1979). External airflow effects on personal sampling. *Annals of Occupational Hygiene*, *22*, 299–310.